GSA Data Repository 2015361

Radiometric dating and temperature history of banded iron formation–associated hematite, Gogebic iron range, Michigan, USA

K.A. Farley and R. McKeon

Methods

The analytical methods used here follow closely those previously described for He and Ne analyses of hematite (Farley and Flowers, 2012). Briefly, approximately 20 grams of sample was crushed with a mortar and pestle and wet-sieved into a 100 – 500 μm size range with the goal of producing a well-homogenized granular sample to source multiple aliquots for various analyses.

Larger pieces of sample material were retained during crushing and used to make polished mounts for secondary electron microscope (SEM) analysis. These analyses showed that the specimens consist entirely of hematite. They also indicate that the samples are polycrystalline aggregates composed of a range of crystallite sizes (Figure DR1).

He and Ne Analysis

At the high temperatures necessary for Ne extraction from hematite (~1250^{o}C), loss of U may occur as it does in goethite (Vasconcelos et al., 2013). For that reason we used a two-aliquot method for He and Ne dating of bulk sample. For the noble gas measurement, between 40 and 60 mg of the 100 – 500 μm size fraction was loaded in a tin ball and placed in the sample introduction system of a double-walled vacuum furnace. Samples were evacuated for at least 12 hours, but were not baked. He and Ne were extracted in one of two ways. In the first method, the sample ball was dropped into the molybdenum furnace crucible and heated to ~1250^{o}C in a single heating step with 30 minutes at the set point. The second method used a 50:50 lithium metaborate:lithium tetraborate flux to extract the noble gases. Approximately 5 grams of flux was

loaded into the molybdenum crucible and degassed at 1000°C for ~30 minutes. After the crucible cooled, the sample was dropped into the crucible and ramped up to 1000˚C over the course of ~20 minutes, where it then was held for an additional 15 minutes. The slow temperature ramp was used to avoid undesirable bubbling and splashing of the flux that results from faster heating. Blanks were measured with both methods both before and after sample analysis. In both methods at least four and sometimes eight samples could be degassed in sequence without breaking vacuum.

There was no noticeable difference in He or Ne concentrations measured by flux fusion compared with ordinary resistance heating (Table DR2). We take this to mean that both methods are quantitatively effective in degassing these hematite specimens.

After extraction, the noble gases were introduced into the vacuum processing line. At this stage the gas was split. Approximately 75% was used for the neon analysis, while 25% was held back for the He analysis. After sequential exposure to hot and cold SAES NP10 getters and a charcoal trap held at liquid nitrogen temperature, the Ne split was adsorbed on charcoal held at 20 K. To separate Ne from the far more abundant He in the sample, the charcoal was heated to 25 K, at which temperature He desorbs and was pumped away while Ne remains trapped. Once the He was removed the charcoal was heated to 68 K to desorb neon, which was introduced into a GV Helix-SFT mass spectrometer. Neon was measured by pulse counting on the high resolution mass-3 spur. Isobaric corrections were obviated as described elsewhere (Farley and Flowers, 2012). Simultaneously with the neon analysis, the vacuum line was pumped, and then the remaining 25% of the gas was processed and analyzed for He abundance on a MAP 215-50 mass spectrometer using standard methods in this laboratory (Amidon et al., 2009).

A manometrically calibrated standard consisting of terrestrial atmosphere doped with He from commercial He cylinders was used to verify instrument sensitivity and isotopic fractionation of Ne. The standard was treated identically to the sample, so inherently includes the split fraction

used for the analyses. In addition to standards and hot blanks (when the furnace was heated to the sample extraction temperature) we also analyzed cold procedural blanks. These measurements provide information on He and Ne introduced from the vacuum line and in the mass spectrometer, and, more importantly, document the presence of trace isobaric species in the neon measurement (Farley and Flowers, 2012). Cold blanks were subtracted from hot blank, sample, and standard analyses. Because hot blanks were found to be indistinguishable from atmospheric Ne, no hot blank correction was made. Instead the abundance of nucleogenic neon (^{21}Ne*) was determined by isotopic deconvolution, assuming an atmospheric endmember with the composition measured on the air standard and a nucleogenic endmember with $^{21}Ne/^{20}Ne=11.5$ (all results would be indistinguishable if we ignored the very tiny amount of nucleogenic ^{20}Ne, as previous workers have done (Farley and Flowers, 2012). No blank corrections were required for the He analyses given the enormous amount of He in the samples. The nucleogenic ^{21}Ne and artificial spallogenic ^{3}He are both many orders of magnitude higher than any conceivable natural production from cosmic ray irradiation of the samples, especially given the very low productivity of ^{21}Ne in Fe_2O_3.

U and Th Analysis

Additional splits of the starting material were analyzed for U, Th and Sm by isotope dilution inductively-coupled plasma mass spectrometry (Farley and Flowers, 2012). Because we are seeking an average parent isotope concentration to compare with the material analyzed for He-Ne, we analyzed aliquots of ~25 mg that were split down prior to isotope dilution and subsequent analysis. Prior to splitting the hematite was dissolved in boiling concentrated HCl for ~12 hours. The resulting solution was then diluted with ultrapure water, split volumetrically, and spiked. The resulting acid concentration was ~6%.

Between 4 and 6 aliquots of each sample were measured for He and Ne on the one hand and for U, Th, and Sm on the other. The abundances of Th and Sm are negligibly small in the age computations. In all cases the standard error of the mean of the U, He, and ^{21}Ne* measurements

was better than a few percent, so all measurements were combined in the age computation. ^{21}Ne ages were computed using the neutron capture production rates of (Gautheron et al., 2006), which are consistent with recent direct experimental verification (Cox et al., 2012). No corrections are required for α or ^{21}Ne ejection in these cm-sized specimens.

^{4}He/^{3}He Analysis

A separate aliquot of ~30 mg was proton irradiated to make a uniform distribution of ^{3}He (Shuster et al., 2003). Samples received a fluence of $4x10^{15}$ protons/cm^2 with an energy of 220 MeV at the Frances Burr Proton Therapy Center at Massachusetts General Hospital. For the simultaneous diffusion and ^{4}He/^{3}He experiments, 0.5 – 4 mg of sample was loaded in a Pt tube that was then spot welded to a thermocouple wire mount and heated with a projector lamp apparatus (Farley et al., 1999) at temperatures below ~500^{o}C, or with a diode laser for higher temperatures. Samples were step-heated, including both prograde and retrograde steps. Evolved gases were purified and analyzed on a MAP 215-50 mass spectrometer, as previously described (Farley and Flowers, 2012). After step heating, the Pt tube was dropped into a double-walled vacuum furnace and heated to 1250˚C to extract and analyze all He remaining in the sample. Cold blanks of equal duration to sample heating steps were run as part of the step heating sequences and were used to correct ^{3}He and ^{4}He yields for each step. ^{3}He yields were converted to diffusion coefficients using standard formulae (Fechtig and Kalbitzer, 1966). ^{4}He/^{3}He data were converted to step ages using the bulk ^{4}He/^{3}He ratio observed for the step heating experiment of each aliquot and the bulk He age of each sample. The uncertainty of the resulting age spectrum was calculated using a Monte Carlo approach that combines the observed uncertainty of the He bulk age, the sensitivity calibration of the mass spectrometer measurements, the cold blank, and the mass spectrometer measurements (listed in order of decreasing contribution).

Domain and Inverse Thermal History Modeling

We used a multiple diffusion domain (MDD) approach described by (Lovera et al., 1991) (renamed a poly-diffusion domain model (Evenson et al., 2014) to indicate the domains are discrete crystallites rather than structures within a crystal) and implemented by (Farley and Flowers, 2012) and (Gallagher, 2012) to model the thermal histories experienced by our samples.

The activation energy (Ea) for each sample was derived from ^{3}He release data by fitting linear regressions to retrograde heating cycles on an Arrhenius plot. For MI-43 and MI-81 where multiple retrograde cycles were measured, we adopted the mean of all retrograde sequences as the Ea of the sample and used it for modeling each aliquot. For MI-45 there was only one retrograde cycle analyzed and the resulting Ea of 184 kJ/mol was used to model that sample. See Table DR4 for details about the derivation of Ea's used for modeling.

With Ea for each sample determined, we modeled the domain size distribution (DSD) individually for each aliquot analyzed by step heating. We fit the observed ln(r/ro) plot (Lovera et al., 1991) by allowing a fixed number of contributing domains and adjusting the relative size and the proportion of the total ^{3}He contained therein. We used an analytical solution for diffusion from a sphere to determine the gas release from each domain using the step heating schedule from a particular aliquot. We then summed the gas release from all contributing domains for each heating step to generate a synthetic ln(r/ro) plot using the standard equations for diffusion coefficients from (Fechtig and Kalbitzer, 1966). We created a program to automate this process and search for the best fit to the observed ln(r/ro) plot given a user specified number of diffusion domains. Eight domains was visually adequate to match the diffusion data. See Figure DR4 for the results of modeling the DSD for each aliquot.

We modeled the thermal histories of our samples using the program QTQt, a Bayesian transdimensional Markov Chain Monte Carlo approach to inverse modeling of thermochronometric data (Gallagher, 2012). This approach favors simple temperature paths

(small number of slope changes) because the misfit between modeled and observed results is weighted by the complexity of the path.

As described in the main text, we favor the idea that our Ne bulk ages indicate formation ages for our hematite samples, and so we use them as a starting point for the inverse modeling. Thermal histories were required to start at the Ne bulk age ± 1σ and between 0 and 250˚C, thermal histories were required to end today between 10 and 30˚C; no other constraints were placed on the inverse model and model thermal histories were allowed to experience heating and cooling at any rate. For MI-81 and MI-43, where multiple step heating experiments were conducted, we simultaneously (jointly) inverted all the available DSD and age spectra data. For MI-45 we inverted the single DSD and age spectrum. Figure DR5 shows the full results from inverse modeling for each sample. A key point regarding the 95% CI curves is that these are bounds on the time-temperature path only; no single path necessarily follows this bound. Thus the 95% CI bounding fits to the $^{4}He/^{3}He$ spectra shown (e.g., in Fig 3c) are not reflective of any single path that fits the data. Instead they are what is predicted on a path that follows the 95% envelope of the temperature paths.

The Ne closure temperature of hematite has not yet been measured. For the two phases for which He and Ne closure temperatures are known (Ol, Qtz (Gourbet et al., 2012; Shuster and Farley, 2005; Shuster et al., 2004)), the neon closure temperature is 150-300^{o}C higher than the He closure temperature. Thus by analogy we infer that the bulk closure temperature of the Ne system in hematite is at least 150^{o}C higher than the bulk He closure temperature in our hematites, or >300^{o}C.

REFERENCES

Amidon, W. H., Rood, D. H., and Farley, K. A., 2009, Cosmogenic He-3 and Ne-21 production rates calibrated against Be-10 in minerals from the Coso volcanic field: Earth and Planetary Science Letters, v. 280, no. 1-4, p. 194-204.

Cox, S. E., Farley, K. A., and Hemming, S. R., 2012, Insights into the age of the Mono Lake Excursion and magmatic crystal residence time from (U-Th)/He and Th-230 dating of volcanic allanite: Earth and Planetary Science Letters, v. 319, p. 178-184.

Evenson, N. S., Reiners, P. W., Spencer, J. E., and Shuster, D. L., 2014, Hematite and Mn oxide (U-Th)/He dates from the Buckskin-Rawhide detachment system, western Arizona: gaining insights into hematite (U-Th)/He systematics: American Journal of Science, v. 314, no. 10, p. 1373-1435.

Farley, K. A., and Flowers, R. M., 2012, (U-Th)/Ne and multidomain (U-Th)/He systematics of a hydrothermal hematite from eastern Grand Canyon: Earth and Planetary Science Letters, v. 359, p. 131-140.

Farley, K. A., Reiners, P. W., and Nenow, V., 1999, An apparatus for high-precision helium diffusion measurements from minerals: Analytical Chemistry, v. 71, p. 2059-2061.

Fechtig, H., and Kalbitzer, S., 1966, The diffusion of argon in potassium-bearing solids., *in* Schaeffer, O. A., and Zahringer, J., eds., Potassium Argon Dating: New York, Springer Verlag.

Gallagher, K., 2012, Transdimensional inverse thermal history modeling for quantitative thermochronology: Journal of Geophysical Research-Solid Earth, v. 117.

Gautheron, C. E., Tassan-Got, L., and Farley, K. A., 2006, (U-Th)/Ne chronometry: Earth and Planetary Science Letters, v. 243, no. 3-4, p. 520-535.

Gourbet, L., Shuster, D. L., Balco, G., Cassata, W. S., Renne, P. R., and Rood, D., 2012, Neon diffusion kinetics in olivine, pyroxene and feldspar: Retentivity of cosmogenic and nucleogenic neon: Geochimica Et Cosmochimica Acta, v. 86, p. 21-36.

Lovera, O., Richter, F., and Harrison, T., 1991, Diffusion domains determined by 39Ar released during step heating: Journal of Geophysical Research, v. 96, p. 2057-2069.

Shuster, D. L., and Farley, K. A., 2005, Diffusion kinetics of proton-induced Ne-21, He-3, and He-4 in quartz: Geochimica Et Cosmochimica Acta, v. 69, no. 9, p. 2349-2359.

Shuster, D. L., Farley, K. A., Sisterson, J., and Burnett, D. S., 2003, He-4/He-3 thermochronometry: Geochimica Et Cosmochimica Acta, v. 67, no. 18, p. A436-A436.

Shuster, D. L., Farley, K. A., Sisterson, J. M., and Burnett, D. S., 2004, Quantifying the diffusion kinetics and spatial distributions of radiogenic He-4 in minerals containing proton-induced He-3: Earth and Planetary Science Letters, v. 217, no. 1-2, p. 19-32.

Vasconcelos, P. M., Heim, J. A., Farley, K. A., Monteiro, H., and Waltenberg, K., 2013, Ar-40/Ar-39 and (U-Th)/He - He-4/He-3 geochronology of landscape evolution and channel iron deposit genesis at Lynn Peak, Western Australia: Geochimica Et Cosmochimica Acta, v. 117, p. 283-312.

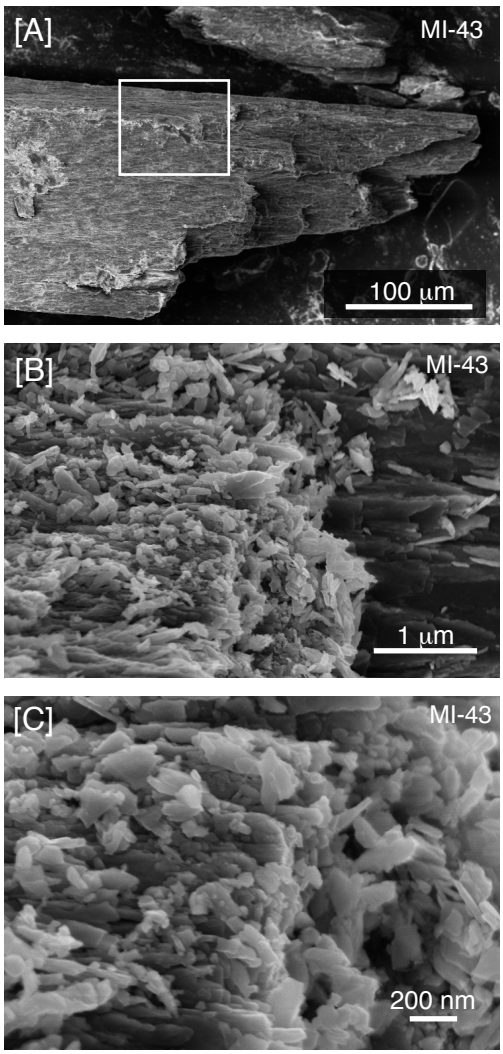

Figure DR1: SEM electron back-scatter images of an unpolished fragment of MI-43 similar in size to those used for diffusion experiments. The images range from 500x to 75,000x magnification and illustrate the polycrystalline nature of these hematite specimens.

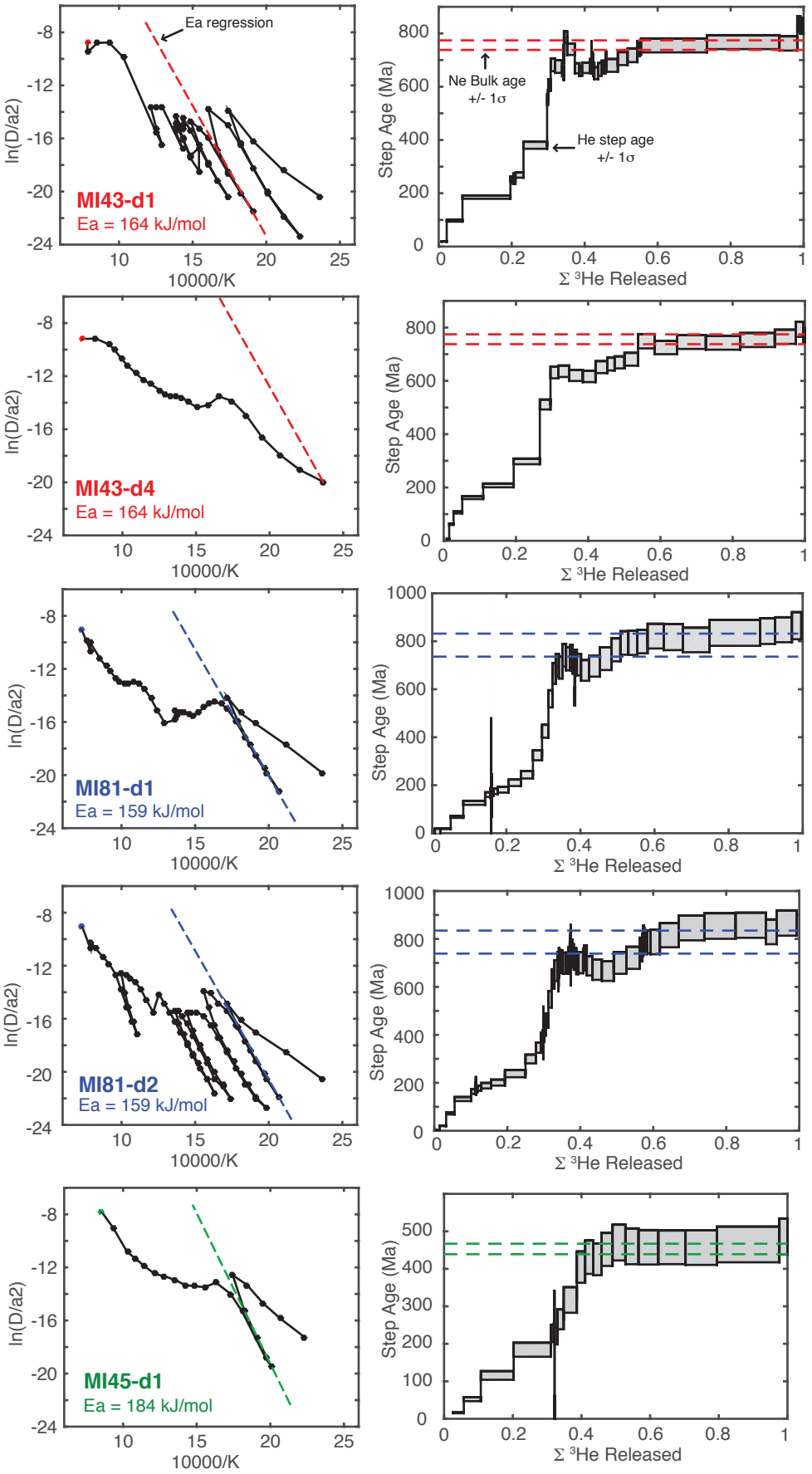
Ea regression
MI43-d1
Ea = 164 kJ/mol
ln(D/a2)
10000/K
Step Age (Ma)
Ne Bulk age
+/- 1σ
He step age
+/- 1σ
Σ ³He Released
MI43-d4
Ea = 164 kJ/mol
MI81-d1
Ea = 159 kJ/mol
MI81-d2
Ea = 159 kJ/mol
MI45-d1
Ea = 184 kJ/mol

Figure DR2: Observed data from the hematite step heating experiments not shown in Figure 2 of the main text. See the caption of Figure 2 for an explanation of the Arrhenius plots (left column) and He age spectra plots (right column). The activation energy used for modeling the domain size distribution for each sample is indicated on the lower right of the Arrhenius plots and illustrated by the colored dashed line; for aliquots in which no retrograde sequence was performed (e.g., MI43-d4) the mean Ea for the other aliquots of that sample were adopted. The quantity ln(r/ro) is schematically depicted on the Arrhenius plot for MI-43-d4, where ln(r/ro) is half the vertical distance to any point in Arrhenius space from a line representing a constant activation energy. See (Farley and Flowers, 2012) for further explanation.

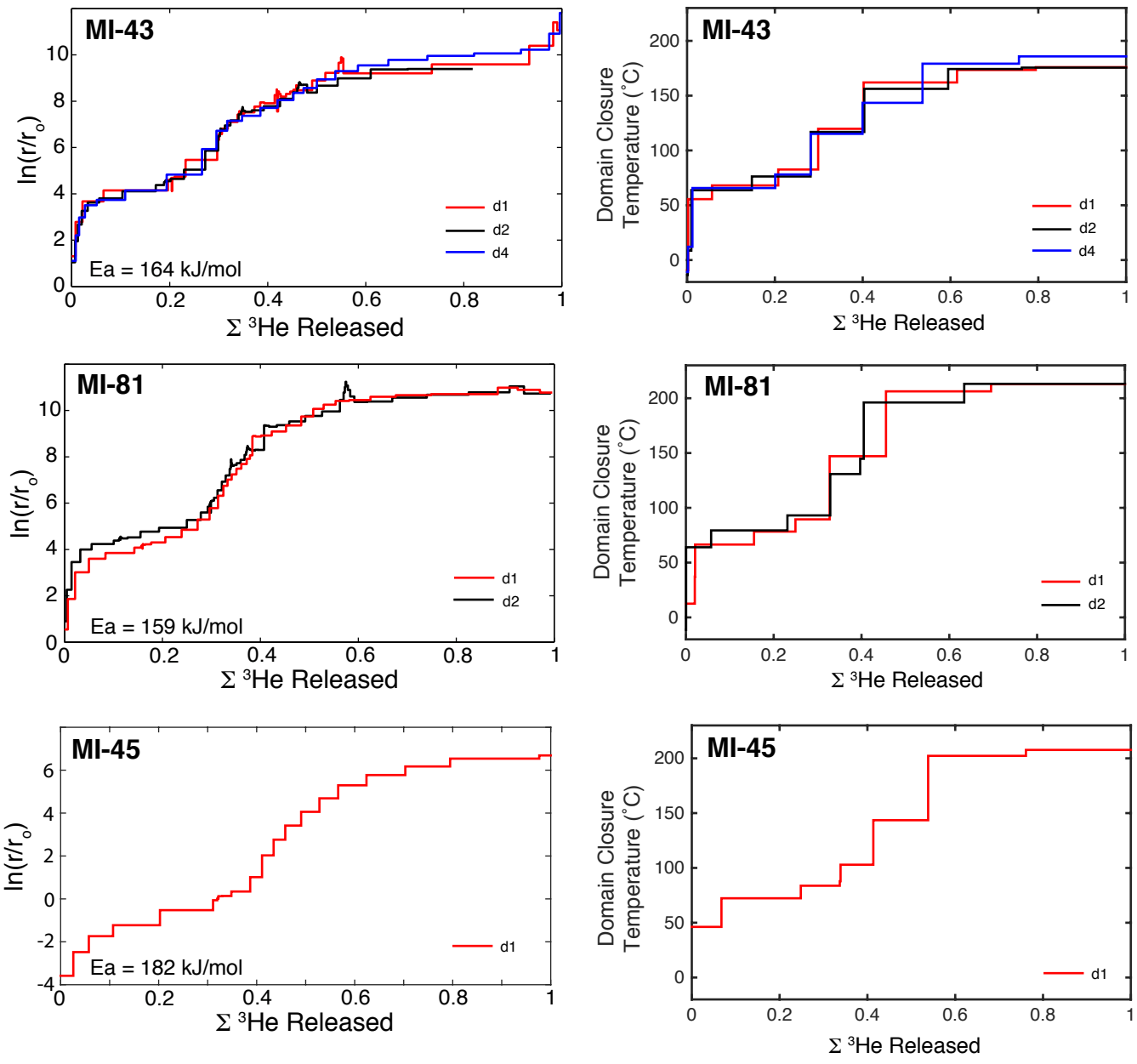

Figure DR3: ln(r/ro) plots (left column) and interpreted domain closure temperature plots (right column) for each step heating experiment from this study. The reproducibility of the diffuson behavior between different step heating experiments from the same sample is clearly illustrated by the ln(r/ro) plots. The inferred domain size distributions (represented through the proxy of domain closure temperature) from modeling the 3He release data are also highly reproducible as indicated by the three aliquots of MI-43.

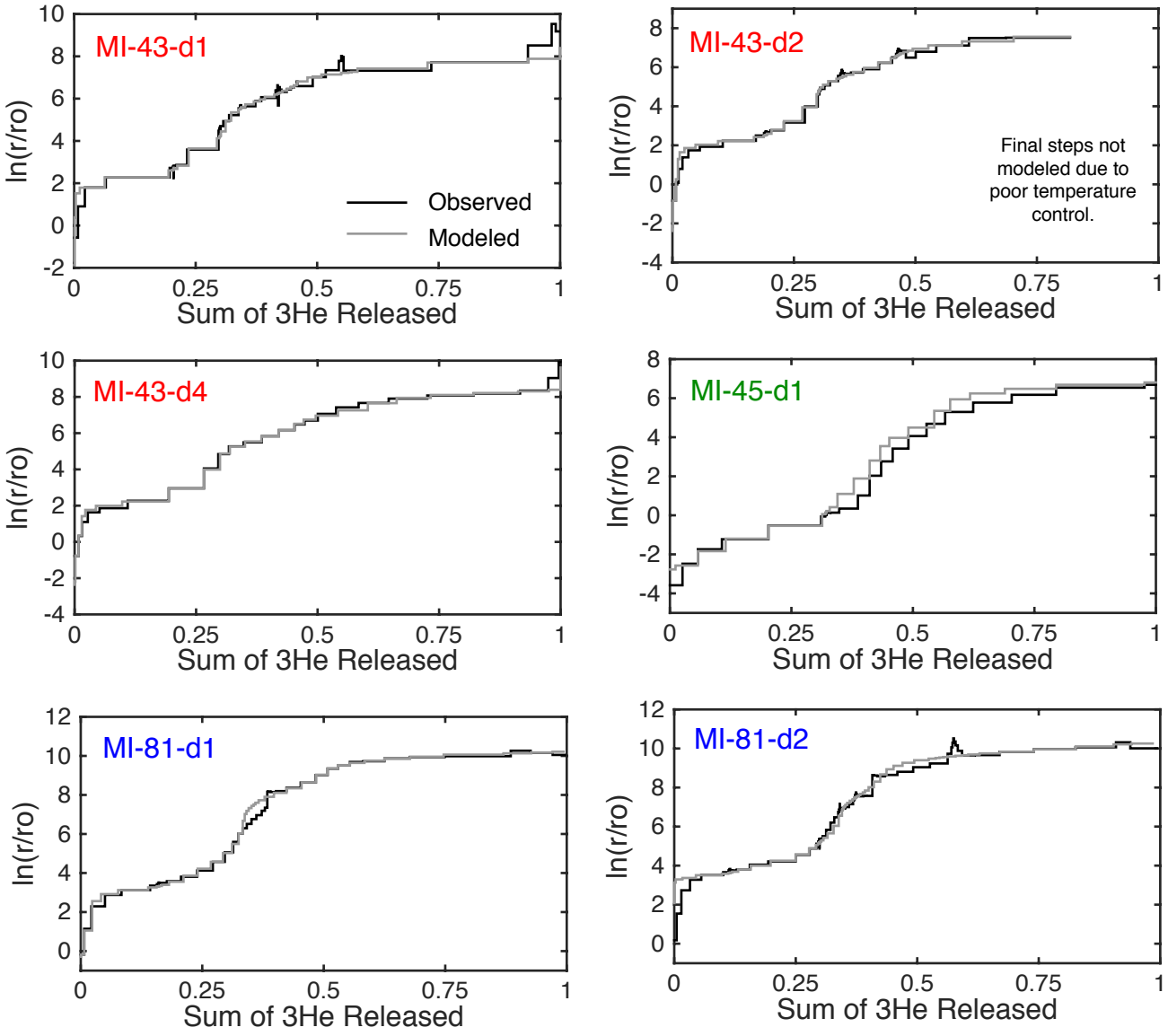

Figure DR4: Plots showing the results of modeling the domain size distribution for each aliquot used in inverse modeling. Observed ln(r/ro) data (black lines) was fit by changing the size and gas fraction of 8 domains the results of which are shown by gray lines.

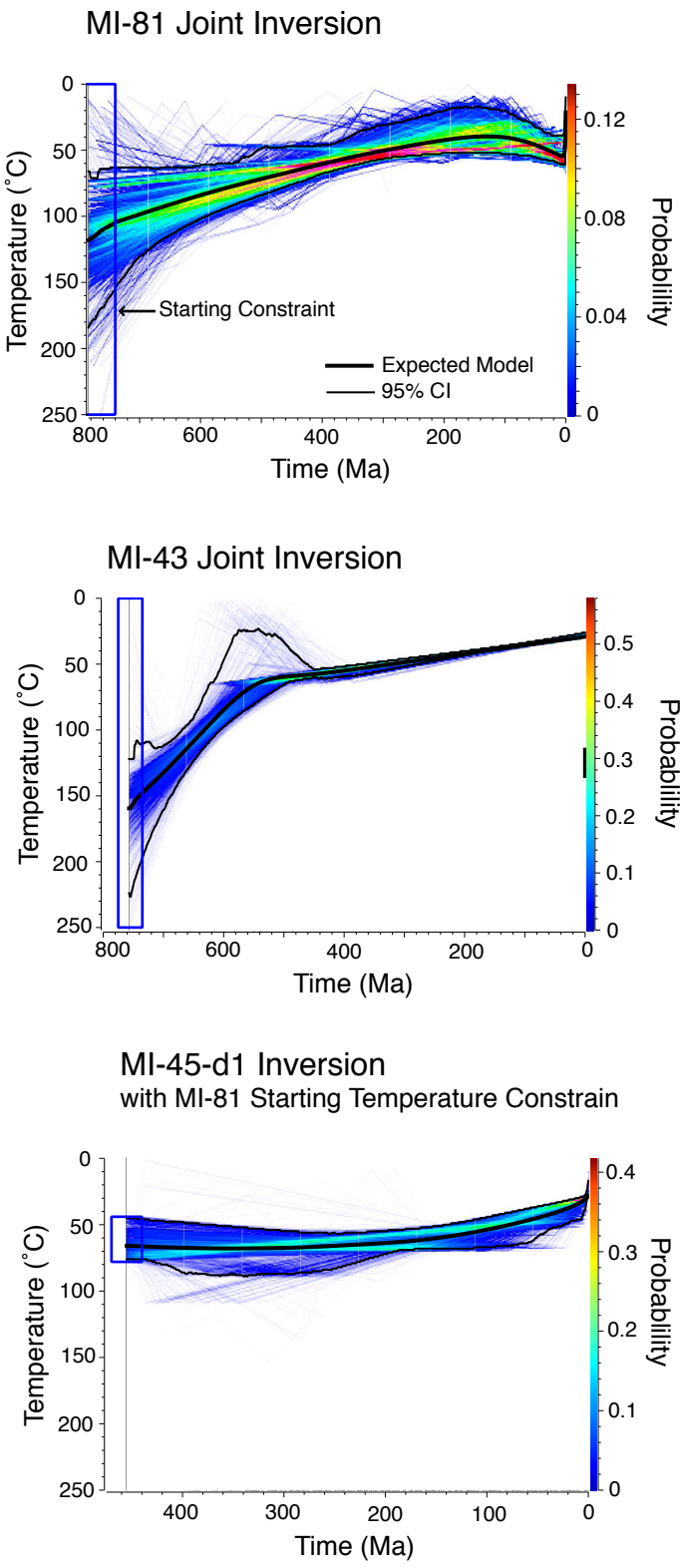

Figure DR5: QTQt expected model temperature history density plots. Here the results of the joint inversion for each sample are shown in greater detail. The time-temperature space shown in each plot is broken down into 1 Ma by 1 ˚C grid cells and the color of each cell indicates the probability that the true thermal history passed through that cell.

Table DR1. Summary Table for Bulk Helium and Neon Age Determination

	Bulk Ages				Daughter Concentrations					Parent Concentrations							
	Helium		Neon		[^{4}He]		[^{21}Ne*]		Nucleogenic	[U]		Th		Sm			
Sampl	(Ma)	±	(Ma)	±	(nmol/g)	±	(fmol/g)	±	^{21}Ne* (%)	(ppm)	±	(ppm)	±	(ppm)	Mine	Lat (oN)	Lon (oW)
MI-43	571	18	756	18	22.8	0.6	0.90	0.02	97	7.00	0.11	0.01	0.01	0.88	Old G Pabst	46.457	90.140
MI-81	595	37	789	48	38.5	0.8	1.53	0.02	98	11.31	0.67	0.12	0.05	1.27	Ashland	46.451	90.169
MI-45	336	10	453	14	13.8	0.1	0.55	0.02	97	7.37	0.06	0.02	0.02	0.43	Ashland	46.451	90.169

Table DR2: He, Ne, U, Th, and Sm data for the aliquots of MI-43, MI-45 and MI-81 that comprise the bulk He and Ne age determinations.

Aliquot	Degassed mass (mg)	[^{4}He] nmol/g	[^{21}Ne*] fmol/g	Nucleogenic ^{21}Ne*(%)	^{21}Ne*/^{4}He
MI-43					
MI43-HeNe1[1]	*48.58*	*23.787*	*0.928*	*97.6*	*3.903E-08*
MI43-HeNe2	52.60	22.846	0.910	97.0	3.983E-08
MI43-HeNe3	58.09	22.465	0.895	96.4	3.984E-08
MI43-HeNe4	52.70	22.212	0.907	96.7	4.083E-08
MI43-HeNe5	51.60	22.176	0.904	97.1	4.076E-08
MI43-HeNe6	53.20	23.173	0.878	97.0	3.789E-08
	Mean	22.777	0.904	97.0	3.969E-08
	SD	0.626	0.017	0.4	1.109E-09
	SD %	2.749	1.844	0.4	2.79
MI-81					
MI81-HeNe1	36.79	38.055	1.536	98.1	4.036E-08
MI81-HeNe2	37.00	38.199	1.553	96.8	4.066E-08
MI81-HeNe3	56.00	37.961	1.511	98.4	3.981E-08
MI81-HeNe4	39.40	39.739	1.532	98.1	3.855E-08
	Mean	38.488	1.533	97.9	3.985E-08
	SD	0.839	0.017	0.7	9.327E-10
	SD %	2.181	1.128	0.7	2.34

Aliquot	Digested Mass (mg)	U (ppm)	+/-	Th (ppm)	+/-	Sm (ppm)
MI-43						
MI43-P1	26.28	6.93	0.02	0.01	0.01	0.81
MI43-P2	26.74	6.89	0.02	0.01	0.01	0.81
MI43-P3	17.19	7.08	0.03	0.01	0.01	1.05
MI43-P4	27.29	7.16	0.03	0.01	0.01	0.86
MI43-P5	23.51	6.97	0.02	0.02	0.01	0.88
	Mean ppm	7.00	0.03	0.01	0.01	0.88
	SD ppm	0.11	0.00	0.01	0.00	0.10
	SD %	1.59	6.06	44.02	20.18	11.36
MI-81						
MI81-P1	24.53	11.77	0.04	0.18	0.01	1.23
MI81-P2	24.23	12.04	0.04	0.14	0.01	1.36
MI81-P3	22.17	11.23	0.04	0.05	0.01	1.34
MI81-P4	24.93	11.27	0.04	0.14	0.01	1.28
MI81-P5	27.57	10.27	0.04	0.09	0.01	1.17
	Mean ppm	11.31	0.04	0.12	0.01	1.27
	SD ppm	0.67	0.00	0.05	0.00	0.08
	SD %	5.97	5.96	42.44	10.47	6.19

MI-45				
MI-45-Ne1	101.75		0.555	96.6
MI-45-Ne2	100.67		0.546	97.5
MI-45-He1	8.60	13.766		
	Mean ppm	13.77	0.55	97.05
	SD ppm		0.01	0.64
	SD %		1.16	0.66

MI-45						
MI45-P1	24.34	7.23	0.03	0.02	0.01	0.46
MI45-P2	5.27	7.52	0.10	0.02	0.03	0.39
	Mean ppm	7.37	0.06	0.02	0.02	0.43
	SD ppm	0.21	0.05	0.00	0.02	0.05
	SD %	2.78	83.18	13.08	98.31	11.51

*21Ne = Nucleogenic 21Ne

♮ = Degassed at 1250oC; all others flux melted using lithium meta- and tetraborate 50/50 flux

Table DR3.1 - MI-43-d1 Step Heating and Domain Model Results

Domain	Relative Size	Gas Fract	log(Do/a2)	Closure Temp	F 3He cum	
1	0.003	0.00243	17.608132	-9.274580511	0.002432	Ea = 39.1 kcal/mol
2	5.385	0.05428	11.025635	55.55686185	0.056711	
3	16.790	0.15094	10.037952	68.08156845	0.207653	
4	56.892	0.09093	8.977964	82.60820553	0.298581	
5	861.956	0.10348	6.6170902	119.7604432	0.402058	
6	10925.421	0.2128	4.4111837	162.0397534	0.614853	
7	20025.308	0.17934	3.8849017	173.4703804	0.794197	
8	22776.718	0.2058	3.7730778	175.9749414	1	

			Observed			Ea = 39.1				Modeled Results			Ea = 39.1
Step	Temp C	time hr	3He Fcum	10000/K	ln(D/a2)	ln(r/ro)	Rstep/Rbulk	err Rs/Rb	Step Age (Ma)	err Step age (M	3He Fcum-M	ln(D/a2)-M	ln(r/ro)-M
1*	100	1	0.0013	26.7989	-23.9798	-1.8774	0.0033	0.0019	1.8877	1.0757	0.0013	-23.9792	-1.8777
2	150	1	0.0078	23.6323	-20.3511	-0.5761	0.0055	0.0003	3.1644	0.1827	0.0032	-22.2700	0.3833
3	200	1	0.0220	21.1349	-18.3989	0.9049	0.0328	0.0005	18.7251	0.6776	0.0115	-19.6336	1.5222
4	250	1	0.0651	19.1150	-16.2109	1.7983	0.1695	0.0022	96.7701	3.2629	0.0628	-16.1959	1.7908
5	300	1	0.1965	17.4474	-13.8769	2.2720	0.3251	0.0043	185.6343	6.3443	0.1942	-13.8973	2.2822
6	275	1	0.2034	18.2432	-16.3461	2.7237	0.4449	0.0061	254.0234	8.8132	0.2030	-16.1057	2.6035
7	250	1	0.2044	19.1150	-18.2252	2.8054	0.4311	0.0073	246.1826	9.3894	0.2044	-17.8952	2.6405
8	225	1	0.2046	20.0743	-20.0580	2.7780	0.4504	0.0252	257.1761	17.0107	0.2046	-19.7966	2.6473
9	200	1	0.2046	21.1349	-21.8525	2.6317	0.5038	0.0999	287.6561	58.3002	0.2047	-21.8613	2.6361
10*	175	1	0.2046	22.3140	-23.3856	2.2382	0.0100	8.1911	0.0100	4717.2126	0.2047	-24.4639	2.7774
11	225	1	0.2048	20.0743	-20.1353	2.8167	0.4427	0.0220	252.7889	14.8539	0.2049	-19.7999	2.6490
12	275	1	0.2103	18.2432	-16.5219	2.8116	0.4279	0.0060	244.3348	8.4653	0.2121	-16.2533	2.6773
13	300	1	0.2324	17.4474	-15.0604	2.8637	0.4697	0.0063	268.1850	9.6349	0.2354	-14.9924	2.8297
14	350	1	0.2971	16.0475	-13.7596	3.5908	0.6657	0.0090	380.1046	13.1264	0.2937	-13.8638	3.6428
15	325	1	0.2996	16.7182	-16.8646	4.4833	0.9668	0.0135	552.0196	19.7203	0.2989	-16.1524	4.1272

16	300	1	0.3000	17.4474	-18.5230	4.5950	0.9896	0.0213	565.0665	22.4624	0.2999	-17.7322	4.1996
17	275	1	0.3001	18.2432	-20.0903	4.5958	1.0547	0.0575	602.2231	38.5611	0.3001	-19.3283	4.2148
18	250	1	0.3001	19.1150	-21.5087	4.4472	0.8159	0.1494	465.9025	86.7293	0.3001	-21.0640	4.2248
19	300	2	0.3010	17.4474	-18.6714	4.6692	1.0029	0.0167	572.6667	20.4586	0.3020	-17.8242	4.2457
20	350	1	0.3069	16.0475	-15.9761	4.6990	1.0614	0.0148	606.0662	21.4486	0.3116	-15.4758	4.4488
21	375	1	0.3188	15.4285	-15.2302	4.9350	1.1951	0.0165	682.3951	24.0885	0.3229	-15.2712	4.9555
22	400	1	0.3383	14.8555	-14.6761	5.2217	1.1835	0.0161	675.7883	23.8067	0.3378	-14.9353	5.3514
23	375	1	0.3414	15.4285	-16.4418	5.5409	1.1603	0.0156	662.5568	23.4813	0.3413	-16.3380	5.4889
24	350	1	0.3422	16.0475	-17.8577	5.6398	1.1777	0.0181	672.4562	24.6452	0.3423	-17.6148	5.5183
25	325	1	0.3424	16.7182	-19.2541	5.6781	1.2638	0.0413	721.6494	33.3457	0.3425	-18.9495	5.5258
26	300	1	0.3424	17.4474	-20.4759	5.5715	1.2960	0.0943	740.0173	58.9666	0.3426	-20.3832	5.5251
27	350	1	0.3431	16.0475	-17.9563	5.6891	1.1373	0.0200	649.3924	24.0066	0.3435	-17.6472	5.5345
28	400	1	0.3520	14.8555	-15.3885	5.5779	1.3759	0.0148	785.6461	21.9797	0.3521	-15.4159	5.5917
29	425	1	0.3729	14.3236	-14.4644	5.6393	1.2965	0.0137	740.3260	21.1106	0.3697	-14.6469	5.7306
30	425	1	0.3849	14.3236	-14.9604	5.8873	1.1722	0.0127	669.3465	18.9713	0.3823	-14.9192	5.8667
31	425	1	0.3929	14.3236	-15.3228	6.0685	1.1540	0.0130	658.9418	18.2787	0.3923	-15.1080	5.9611
32	450	1	0.4144	13.8284	-14.2767	6.0326	1.1752	0.0135	671.0438	19.8679	0.4118	-14.3802	6.0844
33	425	1	0.4182	14.3236	-15.9658	6.3900	1.1988	0.0152	684.5204	19.7081	0.4175	-15.5683	6.1912
34	400	1	0.4190	14.8555	-17.4964	6.6319	1.1727	0.0158	669.5997	19.9631	0.4193	-16.6816	6.2245
35	375	1	0.4193	15.4285	-18.4601	6.5500	1.2847	0.0553	733.5853	37.9291	0.4199	-17.8316	6.2358
36	375	1	0.4211	15.4285	-16.7124	5.6762	0.5637	0.0097	321.8417	11.4387	0.4205	-17.8416	6.2408
37	400	1	0.4221	14.8555	-17.2852	6.5263	1.2308	0.0204	702.7608	26.2754	0.4222	-16.7358	6.2516
38	400	1	0.4230	14.8555	-17.3172	6.5423	1.2199	0.0204	696.5642	26.0869	0.4238	-16.7686	6.2680
39	425	1	0.4265	14.3236	-16.0408	6.4275	1.1646	0.0165	664.9656	24.0757	0.4283	-15.7812	6.2977
40	450	1	0.4374	13.8284	-14.8459	6.3173	1.1396	0.0155	650.7204	22.5354	0.4380	-14.9565	6.3726
41	450	1	0.4458	13.8284	-15.0799	6.4343	1.1648	0.0161	665.0918	23.9324	0.4458	-15.1541	6.4713
42	450	1	0.4524	13.8284	-15.2852	6.5369	1.1806	0.0160	674.1053	23.6327	0.4522	-15.3258	6.5572
43	450	1	0.4580	13.8284	-15.4430	6.6158	1.1791	0.0160	673.2798	24.3150	0.4576	-15.4742	6.6314
44	425	1	0.4594	14.3236	-16.8096	6.8119	1.2369	0.0191	706.2912	25.9185	0.4594	-16.5397	6.6770

45	500	1	0.4908	12.9341	-13.6375	6.5929	1.1910	0.0156	680.0613	24.1655	0.4800	-14.0791	6.8138
46	525	1	0.5177	12.5290	-13.6898	7.0177	1.2355	0.0163	705.4783	24.2273	0.5087	-13.6576	7.0016
47	550	1	0.5446	12.1485	-13.5941	7.3442	1.2577	0.0166	718.1622	25.9426	0.5494	-13.1882	7.1413
48	525	1	0.5496	12.5290	-15.2206	7.7831	1.3048	0.0186	745.0622	26.1372	0.5642	-14.0954	7.2205
49	500	1	0.5510	12.9341	-16.4825	8.0154	1.3006	0.0203	742.6628	27.2061	0.5704	-14.9449	7.2467
50	525	1	0.5543	12.5290	-15.5907	7.9682	1.3062	0.0185	745.8291	26.0902	0.5830	-14.1914	7.2685
51	700	0.25	0.7349	10.2759	-9.8698	7.3245	1.3223	0.0176	755.0539	26.2612	0.7271	-10.0644	7.4218
52	800	0.25	0.9337	9.3184	-8.7650	7.7142	1.3441	0.0177	767.4877	26.2576	0.9338	-8.7441	7.7038
53	900	0.25	0.9825	8.5241	-8.8040	8.5152	1.3351	0.0177	762.3523	26.7123	0.9994	-7.5420	7.8842
54*	1000	0.25	0.9909	7.8545	-9.5187	9.5313	1.4634	0.0197	835.5952	28.8171	1.0000	-7.2371	8.3905
55*	1000	0.25	0.9976	7.8545	-8.8140	9.1790	1.4505	0.0195	828.2278	29.8268			
Fusion*♮		0.25	1.0000				2.1403	0.0316	1222.0814	44.1436			

* = Step not included in Inverse Modeling due to near blank level 4He yield

♮ = Step not included in Domain Size Distribution modeling because of poor temperature control or gas fully exhausted

Table DR3.2 - MI-43-d2 Step Heating and Domain Model Results

Domain	Relative Si	Gas Fraction	log(Do/a2)	Closure Temp	F 3He cum	
1	0.002739	0.001386	18.177145	-13.7129209	0.001386	Ea = 39.1 kcal/mol
2	0.059843	0.008248	15.498303	8.575491282	0.009634	
3	21.91623	0.13793	10.370798	63.75742681	0.147564	
4	64.67149	0.133778	9.4309037	76.2550615	0.281342	
5	1360.268	0.122301	6.7850802	116.8678857	0.403643	
6	15187.98	0.190997	4.6893291	156.2262036	0.59464	
7	40024.78	0.167908	3.8476714	174.3012125	0.762548	
8	42733.94	0.237452	3.7907834	175.5765592	1	

			Observed Results		Ea = 39.1						Modeled Results		Ea = 39.1 kcal/mol
step	temp C	time hr	F 3He cum	10000/K	ln(D/a2)	ln(r/ro)	Rstep/Rbulk	err Rs/Rb	Step Age (Ma	err Step age (Ma)	3He Fcum-M	ln(D/a2)-M	ln(r/ro)-M
1*	50	0.5	0.0000	30.9454	-30.8399	-2.5270	0.0000	0.0000	0.0000	0.0000	0.0000	-31.1276	-2.3832
2*	100	0.5	0.0012	26.7989	-23.3646	-2.1850	0.0000	0.0000	0.0000	0.0000	0.0012	-23.3641	-2.1853
3*	150	0.5	0.0072	23.6323	-19.8296	-0.8369	0.0033	0.7080	1.8832	403.8900	0.0072	-19.8293	-0.8370
4*	175	0.5	0.0127	22.3140	-19.0608	0.0758	0.0121	0.5683	6.8943	324.1014	0.0113	-19.4281	0.2595
5	200	0.5	0.0206	21.1349	-18.1727	0.7918	0.0323	0.0987	18.4649	56.4750	0.0149	-19.1878	1.2993
6	225	0.5	0.0328	20.0743	-17.2711	1.3846	0.0821	0.0130	46.8559	7.5894	0.0247	-17.7926	1.6453
7	250	0.5	0.0563	19.1150	-16.1013	1.7435	0.1700	0.0043	97.0888	4.0021	0.0476	-16.3362	1.8610
8	275	0.5	0.1035	18.2432	-14.7533	1.9273	0.2609	0.0038	148.9894	5.2693	0.0939	-14.9629	2.0321
9	300	0.5	0.1717	17.4474	-13.7922	2.2296	0.3397	0.0050	193.9836	6.8021	0.1676	-13.7692	2.2182
10	280	1	0.1885	18.0783	-15.5761	2.5009	0.3717	0.0132	212.2238	10.2996	0.1877	-15.4183	2.4220
11*	260	1	0.1917	18.7564	-17.1718	2.6315	0.3797	0.1723	216.7835	97.9118	0.1918	-16.9216	2.5064
12*	240	1	0.1924	19.4875	-18.7535	2.7031	0.3817	4.4128	217.9285	2497.9737	0.1928	-18.4017	2.5272
13*	220	1	0.1925	20.2778	-20.2993	2.6984	0.1968	36.2520	112.3715	20864.3253	0.1929	-19.9706	2.5341
14*	250	1	0.1938	19.1150	-18.0404	2.7130	0.3645	5.2883	208.1253	3052.4140	0.1948	-17.6962	2.5410
15	275	1	0.2016	18.2432	-16.2390	2.6701	0.3827	0.0365	218.5099	21.7847	0.2038	-16.0846	2.5929

	16	300	1	0.2293	17.4474	-14.8656	2.7664	0.4307	0.0082	245.9446	9.1237	0.2294	-14.9396	2.8034
	17	325	1	0.2725	16.7182	-14.2338	3.1679	0.5503	0.0082	314.2402	10.8511	0.2672	-14.3784	3.2402
	18	350	1	0.2990	16.0475	-14.5526	3.9872	0.8037	0.0165	458.9072	17.3716	0.2966	-14.4699	3.9459
19*		335	1	0.3023	16.4433	-16.5730	4.6080	0.9817	0.4564	560.5253	262.8788	0.2998	-16.5863	4.6147
20*		320	1	0.3033	16.8591	-17.7143	4.7695	0.9978	105.6694	569.7629	58597.8528	0.3009	-17.6725	4.7486
21*		305	1	0.3037	17.2965	-18.6817	4.8229	0.9298	16.8488	530.9003	9804.9134	0.3014	-18.6089	4.7864
22*		290	1	0.3039	17.7573	-19.6674	4.8624	0.8369	91.5399	477.8776	52744.5226	0.3015	-19.5450	4.8012
23*		275	1	0.3039	18.2432	-20.7389	4.9201	0.8803	4.2964	502.6547	2358.1935	0.3016	-20.5096	4.8054
24*		260	2.5	0.3040	18.7564	-21.7447	4.9180	0.1372	7.5840	78.3230	4371.6260	0.3017	-21.5241	4.8077
25*		285	1	0.3041	17.9163	-20.1238	4.9341	0.8442	12.8196	482.0442	7226.4091	0.3018	-19.8803	4.8124
26*		310	1	0.3045	17.1482	-18.6282	4.9420	1.0049	6.0438	573.7934	3453.6502	0.3023	-18.3935	4.8247
27*		335	1	0.3063	16.4433	-17.1344	4.8887	1.0224	141.4038	583.7790	81026.8464	0.3042	-17.0931	4.8680
28*		360	1	0.3128	15.7940	-15.8619	4.8913	1.0481	0.1370	598.4873	79.8685	0.3099	-16.0025	4.9616
	29	380	1	0.3240	15.3104	-15.2705	5.0714	1.1187	0.0685	638.7589	44.5945	0.3205	-15.3394	5.1059
	30	400	1	0.3407	14.8555	-14.8129	5.2902	1.1258	0.0404	642.8462	30.2548	0.3375	-14.8106	5.2890
31*		385	1	0.3455	15.1941	-16.0081	5.5546	1.1190	0.2691	638.9253	154.5881	0.3440	-15.7195	5.4103
32*		370	1	0.3474	15.5485	-16.9463	5.6751	1.1121	11.8316	634.9803	6663.7494	0.3469	-16.5049	5.4544
33*		355	1	0.3482	15.9198	-17.7836	5.7284	1.0647	96.7901	607.9663	54331.4374	0.3483	-17.2739	5.4736
34*		340	1	0.3485	16.3092	-18.6314	5.7691	1.0210	60.6545	582.9642	34598.6972	0.3489	-18.0578	5.4823
35*		325	1	0.3487	16.7182	-19.5636	5.8328	1.1448	16.4157	653.6847	9204.4252	0.3491	-18.8731	5.4876
36*		300	3	0.3488	17.4474	-20.8866	5.7768	0.5827	10.1930	332.7228	5703.0408	0.3493	-20.3080	5.4876
37*		330	1	0.3490	16.5796	-19.3617	5.8682	1.1063	7.9097	631.6723	4509.8288	0.3497	-18.6050	5.4899
38*		360	1	0.3499	15.7940	-17.6634	5.7920	1.0912	165.4334	623.0447	92636.6297	0.3513	-17.0778	5.4992
	39	390	1	0.3542	15.0795	-16.0740	5.7003	1.0856	0.4562	619.8678	264.3018	0.3573	-15.7379	5.5322
	40	415	1	0.3676	14.5317	-14.9216	5.6631	1.0916	0.0485	623.2764	34.3914	0.3718	-14.8288	5.6167
	41	435	1	0.3920	14.1213	-14.2416	5.7269	1.0662	0.0262	608.8144	25.5252	0.3943	-14.3081	5.7602
	42	455	1	0.4252	13.7334	-13.8243	5.8999	1.0679	0.0204	609.7435	22.3519	0.4233	-13.9614	5.9684
	43	470	1	0.4519	13.4562	-13.9325	6.2267	1.1234	0.0223	641.4576	24.0095	0.4492	-13.9714	6.2462
	44	455	1	0.4602	13.7334	-15.0383	6.5069	1.1183	0.0966	638.5433	59.1834	0.4583	-14.9507	6.4631

45*		435	1	0.4629	14.1213	-16.1522	6.6822	1.1020	21.0179	629.2486	11797.6112	0.4618	-15.8940	6.5531
46*		415	1	0.4638	14.5317	-17.2116	6.8081	1.1374	33.5800	649.4534	18463.3334	0.4632	-16.7655	6.5851
47*		395	1	0.4641	14.9667	-18.2124	6.8805	1.1244	3.9281	642.0217	2167.4186	0.4638	-17.6507	6.5997
48*		380	2	0.4644	15.3104	-18.9283	6.9003	0.9688	56.3144	553.1897	32997.0973	0.4644	-18.3401	6.6062
49*		365	2	0.4646	15.6703	-19.6829	6.9235	0.7700	4.1307	439.6872	2349.5382	0.4647	-19.0642	6.6142
50*		385	2	0.4650	15.1941	-18.7834	6.9423	1.0232	10.8516	584.2525	6283.1961	0.4654	-18.1371	6.6191
51*		400	2	0.4657	14.8555	-18.0859	6.9267	1.0931	18.4540	624.1294	10393.0946	0.4668	-17.4984	6.6329
52*		420	2	0.4677	14.4269	-17.1418	6.8763	1.1037	7.4260	630.2064	4315.9233	0.4698	-16.7092	6.6601
	53	440	2	0.4724	14.0223	-16.2390	6.8230	1.1156	0.2014	637.0289	116.9352	0.4756	-16.0152	6.7111
	54	455	2	0.4804	13.7334	-15.7000	6.8377	1.1503	0.1115	656.8395	67.0133	0.4844	-15.5855	6.7805
	55	525	0.25	0.5006	12.5290	-12.6374	6.4915	1.1635	0.0288	664.3781	27.2381	0.4944	-13.3474	6.8465
	56	575	0.25	0.5429	11.7904	-11.7871	6.7931	1.2253	0.0195	699.6699	24.9507	0.5266	-12.1004	6.9497
	57	625	0.25	0.6101	11.1340	-11.1282	7.1094	1.3061	0.0186	745.7685	25.9259	0.5959	-11.1521	7.1214
	58	675	0.25	0.6858	10.5469	-10.7472	7.4966	1.3343	0.0183	761.8951	26.1138	0.7021	-10.4008	7.3234
	59	725	0.25	0.8182	10.0185	-9.7409	7.5133	1.3343	0.0180	761.8694	27.2862	0.8183	-9.8385	7.5621
60♮	NA		0.25	0.9428	0	0	0	1.3460	0.0180	768.5833	26.5232			
61*♮	NA		0.25	0.9431	0	0	0	1.2865	20.8940	734.5633	11862.8660			
62*♮	NA		0.25	0.9434	0	0	0	1.2821	3.0459	732.0490	1784.1782			
63*♮	NA		0.25	0.9437	0	0	0	1.2987	6.7892	741.5628	3934.6852			
64*♮	NA		0.25	0.9441	0	0	0	1.3099	5.8429	747.9761	3375.7327			
65*♮	NA		0.25	0.9445	0	0	0	1.2878	2.2636	735.3445	1284.1517			
66*♮	Fusion		0.25	1.0000	0	0	0	1.4809	0.0247	845.5775	31.4295			

* = Step not included in Inverse Modeling due to near blank level 4He yield

♮ = Step not included in Domain Size Distribution modeling because of poor temperature control or gas fully exhausted

Table DR3.3 - MI-43-d4 Step Heating and Domain Model Results

Domain	Relative Siz	Gas Fracti	log(Do/a2)	Closure Te	F 3He cum	
1	0.019495	0.00214	17.844371	-10.937	0.002138	Ea = 39.1 kcal/col
2	0.442042	0.01008	15.133291	12.12322	0.012218	
3	123.61809	0.18852	10.240054	65.69825	0.200734	
4	357.79399	0.08093	9.3169518	78.09667	0.281668	
5	5766.2343	0.11791	6.9024333	115.1634	0.399574	
6	34712.144	0.1367	5.343255	143.4505	0.536269	
7	244704.25	0.2196	3.6469348	179.1717	0.755864	
8	340669.18	0.24414	3.3595522	185.8227	1	

			Observed Results			Ea = 39.1				Modeled Results			Ea = 39.1 kcal/mol
step	temp C	time hr	F 3He cum	10000/K	ln(D/a2)	ln(r/ro)	Rstep/Rbulk	err Rs/Rb	Step Age (Ma)	err Step age (Ma	3He Fcum-M	ln(D/a2)-M	ln(r/ro)-M
1*	50	0.75	0.0002	30.9454	-27.7278	-4.0831	3.7187	0.2874	2123.3770	183.1114	0.0000	-31.1684	-2.3628
2*	100	0.75	0.0016	26.7989	-23.1923	-2.2711	0.3638	0.0086	207.7546	8.1632	0.0015	-23.3488	-2.1929
3	150	0.75	0.0083	23.6323	-19.9563	-0.7735	0.0875	0.0018	49.9702	1.8434	0.0082	-19.9827	-0.7603
4	180	0.75	0.0152	22.0677	-19.0777	0.3265	0.0115	0.0010	6.5879	0.5977	0.0147	-19.1420	0.3586
5	210	0.75	0.0271	20.6975	-17.9261	1.0989	0.1092	0.0018	62.3602	2.3536	0.0220	-18.5691	1.4204
6	240	0.75	0.0513	19.4875	-16.6079	1.6303	0.1862	0.0028	106.3450	3.8226	0.0439	-16.8787	1.7657
7	270	0.75	0.1092	18.4111	-14.9501	1.8604	0.2842	0.0039	162.2952	5.7455	0.0979	-15.2130	1.9919
8	300	0.75	0.1937	17.4474	-13.8716	2.2693	0.3641	0.0050	207.8974	7.2207	0.1938	-13.7878	2.2274
9	330	0.75	0.2661	16.5796	-13.5363	2.9555	0.5218	0.0068	297.9304	10.6256	0.2661	-13.5364	2.9556
10	360	0.75	0.2956	15.7940	-14.1834	4.0520	0.8955	0.0124	511.3031	18.6812	0.2992	-14.0582	3.9894
11	390	0.75	0.3175	15.0795	-14.3621	4.8443	1.1057	0.0147	631.3309	21.6916	0.3195	-14.4267	4.8767
12	420	0.75	0.3477	14.4269	-13.9311	5.2710	1.1140	0.0148	636.0817	21.5408	0.3506	-13.8938	5.2524

13	440	0.75	0.3851	14.0223	-13.5802	5.4936	1.0859	0.0145	620.0254	20.5159	0.3844	-13.6777	5.5424
14	460	0.75	0.4203	13.6398	-13.5024	5.8311	1.0801	0.0150	616.7166	21.3832	0.4202	-13.4847	5.8223
15	480	0.75	0.4526	13.2776	-13.4616	6.1670	1.1409	0.0150	651.4422	22.4384	0.4521	-13.4765	6.1745
16	500	0.5	0.4732	12.9341	-13.4105	6.4794	1.1607	0.0156	662.7695	23.9032	0.4713	-13.4834	6.5159
17	525	0.5	0.5004	12.5290	-13.0438	6.6947	1.1722	0.0167	669.3258	22.6564	0.4961	-13.1501	6.7479
18	565	0.5	0.5381	11.9310	-12.6054	7.0638	1.1926	0.0156	680.9454	24.1138	0.5419	-12.4094	6.9658
19	605	0.5	0.5843	11.3876	-12.2519	7.4217	1.3110	0.0175	748.6063	26.8900	0.6034	-11.9256	7.2586
20	645	0.5	0.6463	10.8915	-11.7633	7.6656	1.2692	0.0170	724.7284	24.7106	0.6627	-11.7414	7.6546
21	690	0.5	0.7257	10.3826	-11.2437	7.9064	1.3056	0.0173	745.4706	25.8473	0.7327	-11.3240	7.9466
22	735	0.5	0.8210	9.9192	-10.6723	8.0768	1.3014	0.0171	743.0909	26.2456	0.8210	-10.7330	8.1071
23	780	0.5	0.9166	9.4953	-10.0542	8.1847	1.3191	0.0177	753.1972	26.3887	0.9126	-10.1178	8.2165
24	825	0.5	0.9746	9.1062	-9.6124	8.3466	1.3404	0.0183	765.3496	26.6364	0.9758	-9.5351	8.3080
25	950	0.5	0.9960	8.1756	-9.1681	9.0401	1.3890	0.0197	793.1006	27.8803	1.0000	-7.8789	8.3955
26	1100	0.5	0.9993	7.2825	-9.1946	9.9321	1.3492	0.0189	770.3946	26.5892	1.0000	-8.5709	9.6202
27*♮	1150	0.25	0.9998	7.0267	-8.7446	9.9588	1.5681	0.0244	895.3767	32.4304			
28*♮	1225	0.25	1.0000	6.6749	-7.4686	9.6669	2.1632	0.0794	1235.2084	59.9711			

* = Step not included in Inverse Modeling due to near blank level 4He yield

♮ = Step not included in Domain Size Distribution modeling because of poor temperature control or gas fully exhausted

Table DR3.4 - MI-81-d1 Step Heating and Domain Model Results

Domain	Relative Si	Gas Fractic	log(Do/a2)	Closure Te	F 3He cum	
1	0.04319	0.020338	14.21337	12.5202	0.020338	
2	0.67827	0.000628	11.82141	37.2713	0.020966	Ea = 38.0 kcal/mol
3	10.5352	0.13421	9.438932	66.4959	0.155176	
4	28.128	0.09439	8.585935	78.3152	0.249566	
5	67.0914	0.077893	7.83088	89.4708	0.327459	
6	2909.41	0.128309	4.556602	147.099	0.455768	
7	55446.5	0.239345	1.996465	206.273	0.695113	
8	73534.5	0.304888	1.751231	212.801	1.000001	

			Observed Results			Ea = 38.0				Modeled Results			Ea = 38 kcal/mol
step	temp C	time hr	F 3He cum	10000/K	ln(D/a2)	ln(r/ro)	Rstep/Rbulk	err Rs/Rb	Step Age (M	err Step age (Ma	3He Fcum-M	ln(D/a2)-M	ln(r/ro)-M
1*	100	0.5	0.0006	26.7989	-24.8076	-0.7217	0.0151		8.9525		0.0004	-25.6745	-0.2882
2	150	0.5	0.0071	23.6323	-19.8347	-0.1802	0.0023	0.3188	1.3529	189.2218	0.0071	-19.8297	-0.1827
3	200	0.5	0.0217	21.1349	-17.7046	1.1427	0.0051	0.0268	3.0479	16.0034	0.0235	-17.5273	1.0541
4	250	0.5	0.0498	19.1150	-16.1428	2.2934	0.0310	0.0010	18.4448	1.2390	0.0417	-16.6755	2.5597
5	280	0.5	0.0838	18.0783	-15.3282	2.8774	0.1146	0.0017	68.1679	4.2070	0.0769	-15.4132	2.9199
6	308	0.5	0.1427	17.2073	-14.1549	3.1236	0.2131	0.0030	126.7494	8.5020	0.1388	-14.1569	3.1246
7	285	1	0.1568	17.9163	-15.9689	3.3526	0.2704	0.0042	160.8341	9.9029	0.1560	-15.7890	3.2626
8	260	1	0.1590	18.7564	-17.7403	3.4349	0.2810	0.0308	167.0900	20.6579	0.1589	-17.4787	3.3042
9*	235	1	0.1594	19.6792	-19.4817	3.4233	0.2923	0.5098	173.8265	304.9554	0.1594	-19.2594	3.3121
10*	210	2	0.1596	20.6975	-21.2085	3.3130	0.3342	6.2170	198.7324	3714.7163	0.1596	-21.2082	3.3128
11*	230	2	0.1601	19.8748	-19.8491	3.4200	0.2629	0.8362	156.3837	496.4859	0.1602	-19.6385	3.3147
12*	250	1	0.1611	19.1150	-18.5829	3.5134	0.2642	0.1455	157.1177	87.6408	0.1616	-18.1957	3.3198
13	270	1	0.1649	18.4111	-17.1757	3.4828	0.2838	0.0148	168.8054	13.5254	0.1667	-16.8808	3.3354
14	290	1	0.1772	17.7573	-15.9514	3.4959	0.2929	0.0047	174.1874	11.1137	0.1815	-15.7456	3.3930

15	310	1	0.2062	17.1482	-14.9576	3.5814	0.3044	0.0041	181.0118	11.7890	0.2114	-14.9007	3.5529
16	324	1	0.2393	16.7462	-14.6465	3.8102	0.3534	0.0050	210.1840	13.4667	0.2406	-14.7533	3.8637
17	339	1	0.2718	16.3359	-14.4952	4.1270	0.4091	0.0058	243.3267	15.2659	0.2677	-14.6842	4.2215
18	354	1	0.2964	15.9451	-14.6368	4.5714	0.5465	0.0076	324.9982	20.9888	0.2927	-14.6382	4.5721
19	369	1	0.3136	15.5727	-14.8992	5.0588	0.7146	0.0105	424.9760	26.8912	0.3114	-14.8302	5.0242
20	384	1	0.3245	15.2172	-15.2935	5.5958	0.9420	0.0146	560.2284	35.8047	0.3249	-15.0828	5.4904
21	399	1	0.3331	14.8776	-15.4957	6.0216	1.1183	0.0168	665.0675	43.2352	0.3334	-15.5097	6.0286
22	413	1	0.3417	14.5741	-15.4588	6.2935	1.1777	0.0171	700.4028	46.5689	0.3374	-16.2211	6.6746
23	428	1	0.3513	14.2623	-15.3042	6.5143	1.1603	0.0170	690.0712	45.2132	0.3410	-16.3214	7.0229
24	443	1	0.3613	13.9636	-15.2293	6.7625	1.2480	0.0191	742.2240	47.0233	0.3455	-16.0691	7.1824
25	458	1	0.3724	13.6771	-15.0846	6.9640	1.2218	0.0183	726.6756	47.7075	0.3513	-15.8109	7.3272
26	457	1	0.3790	13.6958	-15.5707	7.1892	1.2407	0.0198	737.8687	46.5658	0.3557	-16.0701	7.4389
27	458	1	0.3838	13.6771	-15.8479	7.3457	1.1993	0.0215	713.2861	47.6838	0.3595	-16.1871	7.5153
28	500	0.5	0.3858	12.9341	-16.0584	8.1614	0.9598	0.0259	570.8143	37.7736	0.3660	-14.9350	7.5997
29	530	0.5	0.3904	12.4510	-15.1713	8.1798	1.2046	0.0216	716.4479	48.5458	0.3783	-14.2692	7.7288
30	560	0.5	0.4018	12.0026	-14.2520	8.1489	1.1814	0.0180	702.5966	44.7234	0.3974	-13.7594	7.9026
31	590	0.5	0.4234	11.5855	-13.5467	8.1952	1.1408	0.0158	678.4550	43.0978	0.4234	-13.3697	8.1066
32	620	0.5	0.4526	11.1963	-13.1517	8.3697	1.1698	0.0153	695.7384	43.1716	0.4543	-13.0939	8.3408
33	650	0.5	0.4835	10.8325	-12.9844	8.6340	1.2231	0.0167	727.3996	47.2931	0.4845	-13.0030	8.6433
34	679	0.5	0.5079	10.5025	-13.1240	9.0193	1.2849	0.0173	764.1563	47.7232	0.5081	-13.1537	9.0342
35	709	0.5	0.5295	10.1817	-13.1672	9.3477	1.3334	0.0185	793.0355	49.0530	0.5292	-13.1908	9.3595
36	738	0.5	0.5538	9.8897	-12.9646	9.5256	1.3345	0.0178	793.6500	50.6213	0.5536	-12.9592	9.5229
37	768	0.5	0.5813	9.6048	-12.7470	9.6893	1.3428	0.0191	798.6409	48.7837	0.5838	-12.6512	9.6414
38	807	0.5	0.6250	9.2580	-12.1593	9.7270	1.3812	0.0188	821.4516	51.6046	0.6250	-12.2124	9.7536
39	847	0.5	0.6768	8.9274	-11.8111	9.8691	1.3748	0.0189	817.6373	54.6470	0.6776	-11.7934	9.8602
40	896	0.5	0.7487	8.5532	-11.2345	9.9385	1.3542	0.0182	805.3849	51.0546	0.7468	-11.2765	9.9595
41	995	0.5	0.8848	7.8855	-10.0474	9.9835	1.4038	0.0190	834.8882	53.8342	0.8698	-10.2113	10.0654
42	995	0.5	0.9257	7.8855	-10.6098	10.2647	1.4157	0.0197	841.9716	53.2483	0.9266	-10.3429	10.1312
43	1045	0.5	0.9710	7.5864	-9.8442	10.1679	1.4260	0.0194	848.0703	52.1159	0.9710	-9.8570	10.1743

44	1095	0.5	0.9962	7.3091	-9.0786	10.0502	1.4544	0.0202	864.9800	56.5530	0.9933	-9.4059	10.2138
Fusion*♮			1.0000				1.5940		947.9892				

* = Step not included in Inverse Modeling due to near blank level 4He yield

♮ = Step not included in Domain Size Distribution modeling because of poor temperature control or gas fully exhausted

Table DR3.5 - MI-81-d2 Step Heating and Domain Model Results

Domain	Relative Size	Gas Fraction	log(Do/a2)	Closure Tem	F 3He cum	
1	0.000753	0.000516	16.949925	-11.418503	0.000516	
2	3.463229	0.056974	9.6245525	64.0264979	0.05749	Ea = 38.0 kcal/mol
3	12.467681	0.173775	8.5119436	79.3785739	0.231265	
4	35.759749	0.097625	7.596726	93.0726163	0.32889	
5	454.493772	0.068076	5.3884591	130.829031	0.396966	
6	1035.77491	0.008114	4.6729842	144.746326	0.40508	
7	14339.05936	0.228852	2.3904736	196.133834	0.633932	
8	30357.80289	0.366068	1.7389743	213.131758	1	

			Observed Results			Ea = 38.0					Modeled Results			Ea = 38 kcal/mol
step	temp C	time hr	F 3He cum	10000/K	ln(D/a2)	ln(r/ro)	Rstep/Rbulk	err Rs/Rb	Step Age (Ma)	err Step age (Ma)	3He Fcum-M	ln(D/a2)-M	ln(r/ro)-M	
1*[a]	60	0.5	0.0000	30.0165	-32.2118		0.2143	4.8761	127.4591	2824.2871				
2*[a]	100	0.5	0.0006	26.7989	-24.8984		-0.0008	0.0297	-0.4767	19.7708				
3	150	0.5	0.0050	23.6323	-20.5493	0.1771	0.0031	0.0008	1.8502	0.4852	0.0007	-24.3629	2.0839	
4	200	0.5	0.0146	21.1349	-18.5040	1.5424	0.0060	0.0004	3.5368	0.3165	0.0029	-21.6774	3.1292	
5	250	0.5	0.0324	19.1150	-17.0245	2.7342	0.0345	0.0006	20.4977	1.3528	0.0168	-18.1399	3.2919	
6	280	0.5	0.0556	18.0783	-16.1267	3.2766	0.1218	0.0017	72.4312	4.4674	0.0446	-16.3087	3.3676	
7	310	0.5	0.1007	17.1482	-14.8228	3.5140	0.2226	0.0029	132.4045	8.4847	0.0980	-14.8123	3.5087	
8	285	1	0.1118	17.9163	-16.5877	3.6620	0.2760	0.0037	164.1642	10.1751	0.1112	-16.4329	3.5846	
9	260	1	0.1136	18.7564	-18.3885	3.7591	0.2897	0.0058	172.2917	10.8261	0.1135	-18.1066	3.6181	
10	235	1	0.1138	19.6792	-20.2040	3.7844	0.3146	0.0196	187.1157	15.9577	0.1138	-19.8845	3.6246	

11	210	2	0.1139	20.6975	-21.9664	3.6919	0.3354	0.0374	199.4840	24.5481	0.1140	-21.8385	3.6280
12	230	2	0.1143	19.8748	-20.5516	3.7712	0.2722	0.0113	161.8858	11.4562	0.1145	-20.2619	3.6264
13	250	1	0.1151	19.1150	-19.2125	3.8282	0.2804	0.0078	166.7353	11.0428	0.1156	-18.8182	3.6311
14	270	1	0.1182	18.4111	-17.7444	3.7672	0.2876	0.0047	171.0551	10.7721	0.1196	-17.4975	3.6437
15	290	1	0.1288	17.7573	-16.4667	3.7536	0.2987	0.0043	177.6268	10.9557	0.1315	-16.3331	3.6868
16	310	1	0.1555	17.1482	-15.3910	3.7981	0.3163	0.0041	188.1247	11.6094	0.1574	-15.3992	3.8022
17	330	1	0.1934	16.5796	-14.8022	4.0474	0.3380	0.0044	201.0016	12.5305	0.1983	-14.7033	3.9980
18	350	1	0.2499	16.0475	-14.1174	4.2138	0.4003	0.0053	238.0765	14.7403	0.2500	-14.1920	4.2511
19	369	0.5	0.2786	15.5727	-13.8832	4.5508	0.5034	0.0067	299.4108	18.2938	0.2774	-13.9324	4.5754
20	355	1	0.2925	15.9198	-15.1983	4.8764	0.5822	0.0078	346.2337	21.0595	0.2913	-15.2051	4.8798
21	340	1	0.2964	16.3092	-16.4304	5.1201	0.6477	0.0094	385.2205	24.5906	0.2958	-16.3090	5.0594
22	325	1	0.2978	16.7182	-17.4417	5.2346	0.6610	0.0118	393.1440	25.3407	0.2975	-17.2230	5.1253
23	310	1	0.2984	17.1482	-18.3401	5.2726	0.6356	0.0159	378.0069	25.1789	0.2982	-18.0987	5.1519
24	295	1	0.2986	17.6010	-19.2575	5.2984	0.6130	0.0315	364.5623	28.6607	0.2985	-18.9889	5.1641
25	280	2	0.2988	18.0783	-20.1737	5.3001	0.7270	0.0412	432.3583	35.5184	0.2988	-19.9107	5.1686
26	265	2	0.2989	18.5822	-21.0166	5.2397	0.6805	0.0598	404.7225	42.7479	0.2989	-20.8852	5.1740
27	250	3	0.2989	19.1150	-21.8861	5.1650	0.5667	0.0556	337.0393	37.8766	0.2989	-21.8872	5.1655
28	230	6	0.2990	19.8748	-22.7582	4.8745	0.3473	0.1320	206.5516	78.7286	0.2989	-23.3809	5.1859
29	250	3	0.2990	19.1150	-21.9965	5.2202	0.3984	0.1232	236.9195	74.1480	0.2990	-21.9075	5.1757
30	270	2	0.2991	18.4111	-20.8877	5.3389	0.7953	0.0592	472.9767	45.0990	0.2991	-20.5606	5.1753
31	290	2	0.2994	17.7573	-19.6949	5.3677	0.6534	0.0226	388.5738	26.9991	0.2995	-19.3266	5.1835
32	310	2	0.3003	17.1482	-18.5366	5.3709	0.6985	0.0126	415.3994	25.7931	0.3008	-18.1977	5.2014
33	330	1	0.3017	16.5796	-17.4375	5.3650	0.6698	0.0117	398.3541	25.7347	0.3026	-17.1756	5.2341
34	350	1	0.3054	16.0475	-16.4544	5.3823	0.7116	0.0103	423.1845	26.1085	0.3069	-16.2826	5.2964
35	370	1	0.3126	15.5485	-15.7525	5.5085	0.7726	0.0102	459.4700	29.2441	0.3154	-15.5845	5.4246
36	390	1	0.3215	15.0795	-15.4993	5.8304	0.9218	0.0132	548.2500	34.0567	0.3279	-15.1454	5.6534
37	405	1	0.3293	14.7460	-15.6081	6.2037	1.0647	0.0149	633.2103	40.3633	0.3384	-15.2723	6.0358
38	420	1	0.3373	14.4269	-15.5388	6.4742	1.1240	0.0147	668.5026	43.0676	0.3451	-15.6963	6.5530
39	400	1	0.3393	14.8555	-16.9101	6.7500	1.1790	0.0177	701.1711	44.7960	0.3467	-17.0841	6.8370

40	380	1	0.3400	15.3104	-17.9894	6.8546	1.1457	0.0271	681.4052	45.4428	0.3473	-18.0757	6.8978
41	360	1	0.3403	15.7940	-19.0041	6.8996	1.1354	0.0482	675.2841	50.6285	0.3475	-19.0361	6.9156
42	340	1	0.3404	16.3092	-20.0062	6.9080	1.0837	0.0831	644.5156	62.8366	0.3476	-20.0428	6.9263
43	320	2	0.3404	16.8591	-21.0093	6.8837	0.9864	0.0939	586.6524	69.1770	0.3477	-21.0889	6.9235
44	300	3	0.3405	17.4474	-22.0564	6.8447	1.1657	0.2094	693.2968	131.8464	0.3477	-22.2395	6.9363
45	320	2	0.3405	16.8591	-21.1554	6.9567	1.1045	0.1188	656.9136	83.1051	0.3478	-21.1056	6.9319
46*	340	1	0.3406	16.3092	-20.5268	7.1683	1.7465	0.2022	1038.7147	137.3030	0.3479	-20.0538	6.9318
47	360	1	0.3408	15.7940	-19.2634	7.0292	1.1011	0.0514	654.8374	50.5345	0.3481	-19.0830	6.9390
48	380	1	0.3413	15.3104	-18.2763	6.9981	1.1508	0.0318	684.3978	47.1032	0.3486	-18.1882	6.9541
49	400	1	0.3426	14.8555	-17.3139	6.9519	1.2080	0.0214	718.4364	44.8640	0.3498	-17.3769	6.9834
50	420	1	0.3459	14.4269	-16.3729	6.8913	1.1943	0.0170	710.2667	44.0779	0.3522	-16.6652	7.0374
51	435	1	0.3515	14.1213	-15.8452	6.9196	1.1855	0.0161	705.0699	46.4463	0.3559	-16.2347	7.1144
52	450	1	0.3596	13.8284	-15.4442	6.9992	1.1750	0.0154	698.8100	44.0480	0.3611	-15.8711	7.2126
53	460	1	0.3679	13.6398	-15.3789	7.1469	1.1764	0.0167	699.6567	43.8363	0.3670	-15.7277	7.3213
54	445	1	0.3710	13.9247	-16.3513	7.3607	1.2107	0.0173	720.0736	45.9714	0.3699	-16.4280	7.3990
55	430	1	0.3723	14.2217	-17.1730	7.4875	1.2380	0.0212	736.2767	46.6808	0.3714	-17.0703	7.4361
56	415	1	0.3730	14.5317	-17.9590	7.5840	1.2878	0.0322	765.9094	51.1223	0.3722	-17.7012	7.4551
57	400	1	0.3733	14.8555	-18.6427	7.6163	1.2108	0.0425	720.0812	50.9958	0.3726	-18.3415	7.4657
58	385	2	0.3736	15.1941	-19.3749	7.6586	1.2977	0.0437	771.8129	54.3045	0.3730	-19.0023	7.4723
59	360	3	0.3737	15.7940	-20.4978	7.6464	1.2998	0.0795	773.0144	67.1438	0.3732	-20.1571	7.4761
60	340	4	0.3738	16.3092	-21.5758	7.6928	1.2920	0.1231	768.4135	90.0342	0.3733	-21.1523	7.4810
61	360	3	0.3739	15.7940	-20.5155	7.6553	1.1233	0.0764	668.0734	61.6739	0.3735	-20.1708	7.4829
62	380	2	0.3741	15.3104	-19.7770	7.7484	1.2629	0.0594	751.0997	57.6470	0.3739	-19.2545	7.4872
63	400	2	0.3746	14.8555	-18.7857	7.6878	1.2510	0.0326	744.0054	49.2653	0.3746	-18.4025	7.4961
64	420	2	0.3759	14.4269	-17.8864	7.6480	1.2338	0.0212	733.7917	46.5403	0.3763	-17.6220	7.5158
65	440	2	0.3789	14.0223	-17.0465	7.6149	1.2611	0.0180	750.0519	47.7107	0.3797	-16.9294	7.5564
66	460	1	0.3822	13.6398	-16.2445	7.5797	1.2291	0.0176	730.9719	47.3873	0.3828	-16.2990	7.6070
67	480	1	0.3890	13.2776	-15.4948	7.5512	1.2050	0.0168	716.6664	45.0271	0.3881	-15.7386	7.6731
68	500	0.5	0.3951	12.9341	-14.8914	7.5779	1.1735	0.0162	697.9343	44.4525	0.3925	-15.2315	7.7480

69	524	0.5	0.4076	12.5447	-14.1356	7.5724	1.1792	0.0162	701.2862	44.2435	0.3999	-14.6820	7.8456
70	550	0.5	0.4107	12.1485	-15.5078	8.6373	1.2017	0.0172	714.7030	44.5444	0.4107	-14.2648	8.0159
71	580	0.5	0.4178	11.7213	-14.6481	8.6160	1.2258	0.0165	729.0027	44.4556	0.4239	-14.0216	8.3027
72	610	0.5	0.4337	11.3231	-13.8070	8.5762	1.1560	0.0152	687.5435	39.8026	0.4368	-13.9985	8.6719
73	639	0.5	0.4592	10.9631	-13.2568	8.6453	1.1296	0.0147	671.7869	42.4046	0.4512	-13.8333	8.9336
74	669	0.5	0.4917	10.6140	-12.9101	8.8058	1.1205	0.0147	666.3857	41.2183	0.4697	-13.5260	9.1137
75	700	0.5	0.5261	10.2759	-12.7321	9.0401	1.1766	0.0149	699.7611	45.0402	0.4938	-13.1876	9.2678
76	729	0.5	0.5625	9.9785	-12.5493	9.2330	1.2131	0.0164	721.4735	46.2045	0.5235	-12.8811	9.3989
77	704	0.5	0.5702	10.2338	-14.0340	9.7313	1.2710	0.0169	755.8905	49.5163	0.5378	-13.5304	9.4794
78	679	0.5	0.5725	10.5025	-15.2020	10.0583	1.3046	0.0185	775.8833	46.7142	0.5455	-14.1138	9.5142
79	655	1	0.5743	10.7741	-16.1911	10.2932	1.3551	0.0230	805.9283	50.2132	0.5540	-14.6804	9.5378
80	630	2	0.5755	11.0724	-17.2096	10.5172	1.3434	0.0225	798.9950	48.7047	0.5629	-15.2983	9.5616
81	660	2	0.5788	10.7164	-16.2077	10.3567	1.3238	0.0186	787.3311	49.7261	0.5787	-14.6805	9.5931
82	690	1	0.5834	10.3826	-15.1826	10.1633	1.3206	0.0189	785.3837	48.4425	0.5919	-14.1097	9.6268
83	730	0.5	0.5922	9.9686	-13.8257	9.8807	1.3241	0.0181	787.4856	47.4791	0.6051	-13.3746	9.6552
84	768	0.5	0.6183	9.6048	-12.6656	9.6486	1.3239	0.0172	787.3707	51.0563	0.6281	-12.7506	9.6911
85	818	0.5	0.6694	9.1646	-11.8499	9.6616	1.3713	0.0182	815.5925	50.1836	0.6703	-12.0246	9.7489
86	877	0.5	0.7399	8.6945	-11.2902	9.8313	1.4222	0.0200	845.8554	51.5504	0.7400	-11.2985	9.8354
87	936	0.5	0.8256	8.2703	-10.7324	9.9581	1.4358	0.0194	853.9114	53.2083	0.8260	-10.7289	9.9563
88	994	0.5	0.9090	7.8917	-10.2156	10.0616	1.4415	0.0193	857.2913	52.4648	0.9040	-10.3040	10.1058
89	994	0.5	0.9384	7.8917	-10.7252	10.3164	1.3955	0.0186	829.9853	51.6487	0.9406	-10.5194	10.2135
90	1095	0.5	0.9932	7.3091	-8.9931	10.0074	1.4571	0.0197	866.5862	52.8717	0.9845	-9.4896	10.2557
91*♮	1200	0.15					1.5480	0.0211	920.6506	58.8368			

* = Step not included in Inverse Modeling due to near blank level 4He yield

♮ = Step not included in Domain Size Distribution modeling because of poor temperature control or gas fully exhausted

Table DR3.6 - MI-45-d1 Step Heating and Domain Model Results

Modeled with Ea = 44 kcal/mol

Domain	Relative S	Gas Fraction	log(Do/a2)	Closure Tem	F 3He cum
1	0.23781	0.067572	15.2174846	46.198135	0.067572
2	3.54058	0.180689	12.8717897	72.304066	0.248261
3	10.2289	0.088786	11.9502808	83.744855	0.337047
4	14.7347	0.00179	11.6332549	87.854923	0.338837
5	52.4802	0.074624	10.5299464	102.91324	0.413461
6	1029.43	0.124908	7.94474681	143.53143	0.538369
7	31475.4	0.222689	4.97399466	202.25395	0.761058
8	41402.9	0.238943	4.73587514	207.66734	1.000001

Modeled with Ea = 38 kcal/mol

Domain	Relative Size	Gas Fraction	log(Do/a2)	Closure Temp	F 3He cum
1	0.049211	0.037314	13.65954392	17.89881021	0.037314
2	0.960189	0.003361	11.07895485	45.83393683	0.040675
3	1.129738	0.094028	10.93771283	47.51566708	0.134703
4	4.399908	0.241886	9.756781109	62.28879389	0.376589
5	67.664914	0.071638	7.382941232	96.42281882	0.448227
6	615.187326	0.104806	5.465653541	129.3814082	0.553033
7	5831.68021	0.216625	3.512080899	169.4314007	0.769658
8	6784.654125	0.230341	3.380612875	172.407082	0.999999

			Observed			Ea = 44.0			Modeled Results				Ea = 44.0 kcal/mol
Step	Temp C	time hr	3He Fcum	10000/K	ln(D/a2)	ln(r/ro)	Rstep/Rbul	err Rs/Rb	Step Age (Ma)	err Step age (M	3He Fcum-M	ln(D/a2)-M	ln(r/ro)-M
1	175	0.5	0.0259	22.3140	-17.2449	-3.5835	0.0071	0.0009	2.3816	0.3745	0.0115	-18.8676	-2.7721
2	210	0.5	0.0575	20.6975	-15.8715	-2.4805	0.0488	0.0011	16.3808	1.6393	0.0575	-15.6861	-2.5732
3	240	0.5	0.1070	19.4875	-14.6759	-1.7385	0.1558	0.0026	52.3019	5.3410	0.1146	-14.4830	-1.8350
4	270	0.5	0.2027	18.4111	-13.3165	-1.2265	0.3443	0.0050	115.5950	11.6239	0.2026	-13.3731	-1.1982
5	300	0.5	0.3110	17.4474	-12.5860	-0.5248	0.5487	0.0076	184.1833	18.7032	0.3133	-12.5584	-0.5386
6	275	0.75	0.3195	18.2432	-15.2731	-0.0622	0.6786	0.0121	227.8097	22.9441	0.3200	-15.5148	0.0586
7	250	1.25	0.3212	19.1150	-17.3439	0.0079	0.6853	0.0277	230.0716	24.3466	0.3213	-17.5965	0.1342
8	225	2	0.3216	20.0743	-19.4866	0.0171	0.8721	0.1151	292.7504	48.3807	0.3216	-19.7505	0.1491
9*	200	3	0.3216	21.1349	-21.9157	0.0573	2.4635	46.1686	826.9818	15003.0406	0.3216	-22.1045	0.1517
10	235	1.25	0.3220	19.6792	-18.8286	0.1255	0.0779	0.1016	26.1605	34.5335	0.3220	-18.8884	0.1554
11	280	0.75	0.3299	18.0783	-15.3045	0.1360	0.6586	0.0120	221.0890	22.5399	0.3287	-15.4695	0.2186
12	305	0.5	0.3484	17.2965	-13.9899	0.3443	0.7900	0.0124	265.2074	26.4148	0.3448	-14.1338	0.4162

13	340	0.5	0.3868	16.3092	-13.1437	1.0143	0.9441	0.0124	316.9466	34.1517	0.3783	-13.3072	1.0961
14	370	0.5	0.4110	15.5485	-13.4863	2.0279	1.2053	0.0174	404.6048	41.8128	0.4110	-13.1999	1.8847
15	400	0.5	0.4346	14.8555	-13.4184	2.7612	1.2840	0.0189	431.0341	44.5540	0.4327	-13.5073	2.8057
16	430	0.5	0.4583	14.2217	-13.3274	3.4175	1.2675	0.0184	425.5084	42.4438	0.4514	-13.5801	3.5438
17	470	0.5	0.4907	13.4562	-12.9152	4.0589	1.3453	0.0188	451.6089	43.9531	0.4907	-12.7337	3.9682
18	510	0.5	0.5280	12.7689	-12.6502	4.6874	1.4001	0.0191	470.0207	47.6896	0.5439	-12.2660	4.4952
19	550	0.5	0.5663	12.1485	-12.4910	5.2948	1.3704	0.0193	460.0474	47.8315	0.5766	-12.6026	5.3506
20	600	0.5	0.6240	11.4528	-11.9070	5.7730	1.3627	0.0194	457.4731	45.9845	0.6176	-12.2453	5.9421
21	650	0.5	0.7033	10.8325	-11.3341	6.1734	1.3623	0.0182	457.3290	44.9048	0.6892	-11.4759	6.2443
22	700	0.5	0.7947	10.2759	-10.8325	6.5388	1.3607	0.0182	456.8028	46.3200	0.7947	-10.7164	6.4807
23	800	0.5	0.9766	9.3184	-9.0095	6.6875	1.3854	0.0186	465.0691	47.6756	0.9766	-9.0094	6.6874
24	900	0.5	1.0000	8.5241	-7.7788	6.9516	1.4484	0.0201	486.2269	48.1438	1.0000	-7.4884	6.8064
25*♮	900	1	1										

* = Step not included in Inverse Modeling due to near blank level 4He yield

♮ = Step not included in Domain Size Distribution modeling because of poor temperature control or gas fully exhausted

Table DR4 - Activation Energy Estimation

Ea estimates for sample with multiple retrograde heating cycles

MI-43

retrograde cycle	slope	ln(Do/a2)	Ea (kJ/mol)	range of steps regressed
MI-43-d1				
1st	-1.858	17.331	154.5	7-13
2nd	-1.813	13.066	150.7	16-20
3rd	-1.974	13.837	164.1	24-28
MI-43-d2				
1st	-1.941	19.102	161.4	11-16
2nd	-1.989	15.57	165.3	21-28
3rd	-2.053	14.829	170.7	33-41
4th	-2.077	12.835	172.7	47-54
MI-43-d5	Not reported here, but used to estimate Ea			
1st	*-2.050*	*22.305*	*170.5*	*7-14*
MI-43-d6	Not reported here, but used to estimate Ea			
1st	*-1.994*	*20.947*	*165.8*	*7-14*
		mean	164.0	
		SD	7.4	

MI-81

retrograde cycle	slope	ln(Do/a2)	Ea (kJ/mol)	range of steps regressed
MI-81-d1				
1st	-1.848	16.918	153.66	7-14
MI-81-d2				
1st	-1.904	17.318	158.26	6-14
2nd	-1.828	12.916	151.98	20-31
3rd	-2.016	12.741	167.58	37-48
4th	-1.975	10.634	164.21	54-62
		mean	159.1	
		SD	6.7	